THE JOURNAL OF PHYSICAL CHEMISTRY LETTERS
A JOURNAL OF THE AMERICAN CHEMICAL SOCIETY

pubs.acs.org/JPCL

Letter

Understanding the Reaction Dynamics on Heterogeneous Catalysts Using a Simple Stochastic Approach

Bhawakshi Punia, Srabanti Chaudhury,*,§ and A. B. Kolomeisky*,§

Cite This: J. Phys. Chem. Lett. 2021, 12, 11802−11810

Read Online

ACCESS | Metrics & More | Article Recommendations | Supporting Information

ABSTRACT: Recent experimental advances on investigating nanoparticle catalysts with multiple active sites provided a large amount of quantitative information on catalytic processes. These observations stimulated significant theoretical efforts, but the underlying molecular mechanisms are still not well-understood. We introduce a simple theoretical method to analyze the reaction dynamics on catalysts with multiple active sites based on a discrete-state stochastic description and obtain a comprehensive description of the dynamics of chemical reactions on such catalysts. We explicitly determine how the dynamics of catalyzed chemical reactions depend on the number of active sites, on the number of intermediate chemical transitions, and on the topology of underlying chemical reactions. It is argued that the theory provides quantitative bounds for realistic dynamic properties of catalytic processes that can be directly applied to analyze the experimental observations. In addition, this theoretical approach clarifies several important aspects of the molecular mechanisms of chemical reactions on catalysts.

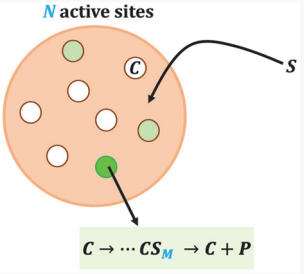

It is impossible to imagine modern industrial processes or scientific research activities without use of catalysts that accelerate the required chemical processes.[1−3] Despite the importance of catalysis and many years of intensive studies, however, the molecular mechanisms of catalytic phenomena still remain not well-understood.[3,4] Significant progress in development of experimental methods for probing the catalytic processes has been achieved in recent years. This is mostly due to the developments of various single-molecule techniques that allowed researchers to uncover the molecular properties of catalytic systems, which are hidden in the ensemble-averaged bulk measurements.[5,6]

Single-molecule fluorescence microscopy experiments investigated the chemical transformations of nonfluorescent reactants into fluorescent products when single nanoparticles (NPs) have been used as catalysts.[5,7] This allowed researchers to achieve excellent spatial and temporal resolutions. The stochastic fluorescent bursts associated with the product formation events were attributed to single catalytic turnovers, and the distributions of waiting times for such events have been measured. The real-time observations of single catalytic turnovers on a single NP catalyst showed that there are wide distributions in the effective rates for the product formation and dissociation and that there are also strong fluctuations in the time-dependent chemical activity.[5,7−9] It has been argued that in a single NP, the intrinsic structural heterogeneity among the different active sites is responsible for such time-dependent fluctuations in the rates of catalytic product formation and dissociation. In addition, it was found that the temporal dependence of the catalytic activities is determined by the size of nanoparticles which can affect the dynamic surface restructuring.[10,11] The study of catalysis using single-molecule fluorescence microscopy has been also successful in revealing the kinetic mechanisms for several specific enzymatic systems.[12,13] Furthermore, these experimental methods have been used recently to investigate the single-molecule kinetics of chemical reactions on gold nanoparticles, uncovering hidden kinetic intermediates that are masked in ensemble-averaged studies.[14]

Single-molecule experimental studies of chemical processes on catalysts have collected a large amount of quantitative information, which stimulated the development of various theoretical methods.[6] The earliest theoretical attempt was based on a Langmuir−Hinshelwood approach that assumes the binding/unbinding equilibrium between the substrates and the catalyst and views all active sites as a single "effective" catalytic site.[15] However, this approach could not explain the experimentally observed size-dependent catalytic activity, and because of its mean-field nature it also failed to account for various stochastic effects.[11] A more advanced theoretical method based on first-passage analysis of chemical dynamics,[16,17] which could partially take into account the number of active sites and the related stochastic effects, was proposed later.[18,19] But this method was also too simplified in many aspects because it did not consider the details of the underlying chemical reactions or the number of intermediates for the chemical processes at each active site. Recently, we developed a new general theoretical framework for investigating the

Received: October 30, 2021
Accepted: December 1, 2021
Published: December 3, 2021

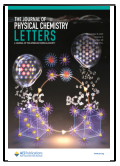

https://doi.org/10.1021/acs.jpclett.1c03557
J. Phys. Chem. Lett. 2021, 12, 11802−11810

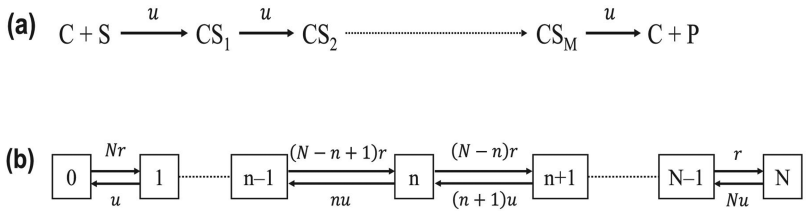

Figure 1. Schematic representation of chemical processes on heterogeneous catalysts with N identical active sites. (a) A sequential chemical reaction with M intermediates. (b) Overall effective chemical kinetic scheme for the whole catalytic particle. Each discrete state n corresponds to the state of the system with n ($0 \le n \le N$) active sites in the chemical conformation (CS_M) just before making the product. For transitions between the states, the effective rate constant is $r = \frac{u}{M}$.

dynamics of chemical reactions with intermediate states on catalytic particles with multiple active sites.[20] It utilized a discrete-state chemical kinetic approach that takes into account the stochasticity of individual chemical reactions at each catalytic site on a single NP.[20,21] The main idea of this method is to follow the dynamics of only those active sites that are just one step before making the final product. This allows better connection with experimental observations and it also significantly decreases the complexity of mathematical calculations of dynamic properties because the originally very complicated multistate system can now be described as a much simpler one-dimensional sequence of effective chemical kinetic "states."[20]

Using this discrete-state stochastic approach, it was explicitly shown that the mean reaction times are inversely proportional to the number of active sites irrespective of the details of underlying chemical reactions.[20] It was also found that the higher moments of reaction times are affected by the details of the chemical reactions at each active site. However, a comprehensive description of the reaction dynamics on a multisite catalyst has been obtained only for the simplified situations with $N = 1$, 2, and 3 active sites, while in real systems even on the smallest nanoparticles the number of active sites is significantly larger (probably $N \approx 10-1000$). This observation limits the applicability of the discrete-state stochastic framework for understanding the mechanisms of catalytic processes.

In this Letter, we develop a simple discrete-state stochastic model of the catalytic chemical reactions on particles with multiple active sites, which can be solved analytically for any number of active sites and for all ranges of relevant parameters. It allows us to obtain a comprehensive explicit description of the reaction dynamics on heterogeneous catalysts and to make the connections between the molecular processes and the observed dynamic features. Our analysis explicitly shows the dependence of the dynamics of catalyzed chemical reactions on the number of active sites, number of intermediate chemical species, and topology of underlying chemical reactions. It is argued that the calculated dynamic properties present quantitative bounds for dynamic properties measured in experiments, clarifying many aspects of molecular mechanisms for chemical reactions on catalysts.

To obtain a comprehensive description of dynamic properties of catalyzed chemical reactions, let us consider a single nanoparticle with N active sites that might catalyze only one specific chemical reaction. Each active site is independent of each other, and for every chemical reaction there are M intermediate states, as schematically shown in Figure 1a. In this process, the substrate molecule S binds to the catalytic site (labeled as C in Figure 1a) to create the complex CS_1 that sequentially transitions through the M intermediate states CS_j ($1 \le j \le M$). From the last complex CS_M, the final product P can be achieved that also releases the catalytic site for a new chemical process. All these transitions are irreversible and assumed to be happening with the same rate u (which sets the time scale in the system). Please note that the first transition (binding of the substrate) is different from other transitions and its rate is concentration-dependent, but for convenience we assume that all transition rates are the same.

Using the idea of the mapping of multiple chemical reactions catalyzed on N active sites of the single NP on a sequence of effective discrete states,[20] the effective chemical kinetic scheme for the whole catalyst with the sequential reaction is presented in Figure 1b. The chemical processes on the single catalyst with N active sites can be viewed as a sequence of stochastic transitions between $N + 1$ discrete states. Each state n ($0 \le n \le N$) corresponds to the effective chemical kinetic state of the system with exactly n active sites in the conformation CS_M. This happens after M intermediate transitions at the given site are already accomplished ($CS_j \rightarrow CS_{j+1}$), and the system is ready for the final transition to make the product molecule at the given site (Figure 1a). From the state n, the final product can be made with the effective rate nu because all active sites are independent. This also moves the system back into the state $n - 1$ because the active site where the product was made is not in the CS_M conformation anymore. The effective forward transition ($n \rightarrow n + 1$) in this kinetic scheme is taking place with a rate $(N - n)r = (N - n)u/M$ (Figure 1b), where the effective rate constant r for transitions between discrete states (Figure 1b) is given by

$$r = \frac{u}{M} \tag{1}$$

This effective forward rate r can be explained using the following arguments. In our simplified model, all intermediate chemical states are equally probable, and the transition to CS_M will occur only from the chemical state CS_{M-1}. There are M possible intermediate chemical states that did not reach yet the state CS_M (*i.e.*, C, CS_1, CS_2, ..., CS_{M-1}). This means that the probability to find the system in the chemical state CS_{M-1} from which the transition will happen is $1/M$. At the same time, for the effective state n there are $(N - n)$ active sites that did not yet reach the conformation CS_M.

This simplified theoretical model provides a minimal description of chemical reactions on catalysts with multiple active sites. It neglects the backward transitions, but in a real system, they are expected to be smaller than the forward transitions, making our simple theory reasonable enough from the experimental point of view. For simplicity, it is also assumed that $u = 1$ because it determines only the time scale in the system.

https://doi.org/10.1021/acs.jpclett.1c03557
J. Phys. Chem. Lett. 2021, 12, 11802−11810

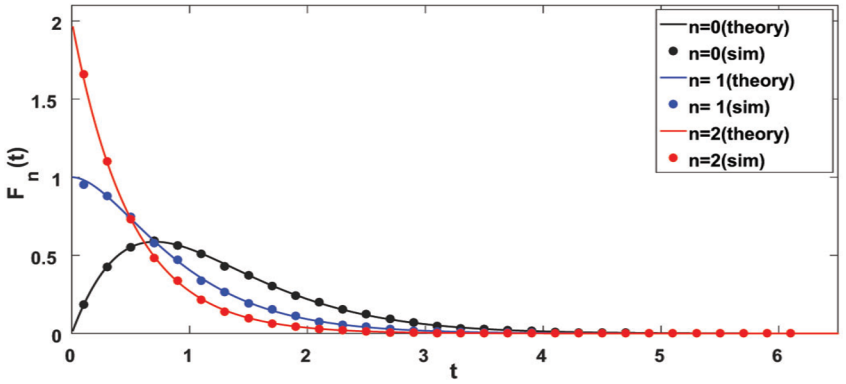

Figure 2. Chemical reaction time distributions for a system with $N = 2$ and $M = 1$, showing results for $n = 0$ (black), $n = 1$ (blue), and $n = 2$ (red). The solid lines are the theoretical predictions obtained by taking inverse Laplace transforms, and the symbols are from Monte Carlo simulations.

To analyze the dynamic properties of the system, we employ a powerful method of first-passage probability densities that was successfully utilized in analyzing various problems in chemistry, physics, and biology.[22−25] This is also stimulated by experimental observations that count the catalytic cycle as soon as the product molecule is created for the first time at the given active site. For this purpose, one can define a function $F_n(t)$ as a probability density function to complete the catalytic cycle at time t starting at the state n at time $t = 0$. The temporal evolution of these first-passage probability densities is governed by a set of backward master equations[20,22]

$$\begin{aligned}
\frac{dF_0(t)}{dt} &= \frac{N}{M}F_1(t) - \frac{N}{M}F_0(t)\\
\frac{dF_1(t)}{dt} &= \frac{N-1}{M}F_2(t) + F_P(t) - \left(\frac{N-1}{M}+1\right)F_1(t)\\
&\cdots\\
\frac{dF_n(t)}{dt} &= \frac{N-n}{M}F_{n+1}(t) + nF_P(t) - \left(\frac{N-n}{M}+n\right)\\
&\quad F_n(t)\\
\frac{dF_N(t)}{dt} &= NF_P(t) - NF_N(t)
\end{aligned} \tag{2}$$

where $F_P(t)$ is for the product state with $F_P(t) = \delta(t)$. This physically means that if the system starts in this state, the process is immediately accomplished.[20]

This set of backward master equations can be analyzed in the Laplace space $[\widetilde{F_n}(s) = \int_0^\infty e^{-st}F_n(t)dt]$ with the initial condition $F_n(t = 0) = 0$, which yields

$$\begin{aligned}
\left(s+\frac{N}{M}\right)\widetilde{F_0}(s) &= \frac{N}{M}\widetilde{F_1}(s)\\
\left(s+\frac{N-1}{M}+1\right)\widetilde{F_1}(s) &= 1+\frac{N-1}{M}\widetilde{F_2}(s)\\
&\cdots\\
\left(s+\frac{N-n}{M}+n\right)\widetilde{F_n}(s) &= n+\frac{N-n}{M}\widetilde{F_{n+1}}(s)\\
(s+N)\widetilde{F_N}(s) &= N
\end{aligned} \tag{3}$$

Solving these equations leads to the explicit expression for the first-passage probability density functions in a compact form:

$$\widetilde{F_n}(s) = \frac{n + \sum_{i=1}^{N-n}(n+i)\prod_{j=1}^{i}\frac{\frac{N-n-(j-1)}{M}}{s+n+j+\frac{N-n-j}{M}}}{s+n+\frac{N-n}{M}} \tag{4}$$

Alternatively, the same result can be written as

$$\widetilde{F_n}(s) = \frac{\left(n+\frac{N-n}{M}\right) - s\sum_{i=0}^{N-n-1}\prod_{j=0}^{i}\frac{\frac{N-n-j}{M}}{s+n+j+1+\frac{N-n-j-1}{M}}}{s+n+\frac{N-n}{M}} \tag{5}$$

These expressions for the first-passage probability density functions are crucial because they allow us to obtain a full dynamic description of chemical reactions on multisite catalysts for a general set of parameters and conditions.

By inverting the explicit Laplace transformation expressions (see eq 5), one can obtain the distributions of first-passage times to make a product molecule starting from any effective chemical state n. The results for the simplest model with $N = 2$ and $M = 1$ are presented in Figure 2 to illustrate this approach. One can see that the distributions of first-passage times depend on the starting state of the system. Distributions that start initially from the state $n = 0$ $[F_0(t)]$ are always non-monotonic because to reach the final product the system must first pass several intermediate states. However, if the process starts from the other states $[F_{n>0}(t)]$, then the distributions should have a more complex shape, starting from a finite value at $t = 0$ (see Figure 2).

Using our theoretical model, more specific dynamic information on underlying molecular mechanisms can be obtained. For example, we can explicitly estimate the mean reaction time (catalytic turnover times) and second moment of the reaction time. But these calculations involve several steps. Expanding $\widetilde{F_n}(s)$, we obtain

$$\widetilde{F_n}(s) \simeq 1 - s\langle T_n\rangle + \frac{1}{2}\langle T_n^2\rangle s^2 - \cdots \tag{6}$$

where $\langle T_n\rangle$ is the mean first-passage time and $\langle T_n^2\rangle$ is the second moment of the first-passage time if starting from the state n. Then from eq 5 it can be shown that

$$\langle T_n\rangle = -\left(\frac{\partial\widetilde{F_n}(s)}{\partial s}\right)_{s=0} = \frac{1+\frac{N-n}{M}\langle T_{n+1}\rangle}{\frac{N-n}{M}+n} \tag{7}$$

and we explicitly obtain

https://doi.org/10.1021/acs.jpclett.1c03557
J. Phys. Chem. Lett. 2021, 12, 11802−11810

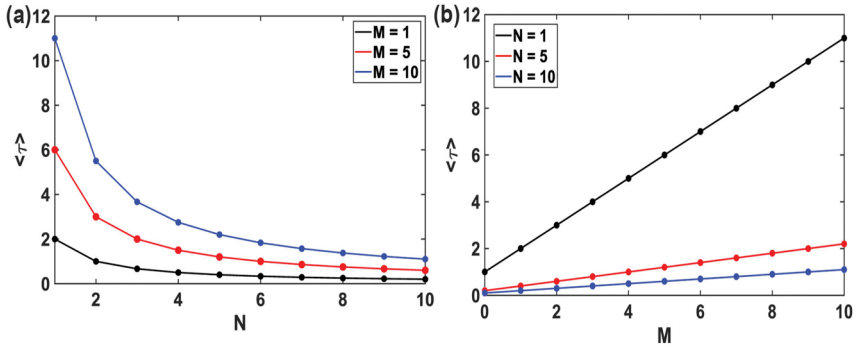

Figure 3. Mean reaction times as a function of (a) the number of active sites N for $M = 1$ (black line), $M = 5$ (red line), and $M = 10$ (blue line) intermediate chemical conformations and (b) the number of intermediates M for $N = 1$ (black line), $N = 5$ (red line), and $N = 10$ (blue line) active sites. The solid lines are the theoretical predictions, and the symbols are from Monte Carlo simulations.

$$\langle T_n \rangle = \frac{1 + \sum_{k=0}^{N-n-1} \prod_{j=0}^{k} \frac{\frac{N-n-j}{M}}{n+j+1+\frac{N-n-j-1}{M}}}{n + \frac{N-n}{M}} \tag{8}$$

One could also obtain $\langle T_N \rangle = \frac{1}{N}$, which can be easily explained. In the state N, all active sites are in the conformation CS_M just before making the product. The probability that the reaction will be accomplished from any active site is equal to $1/N$ and the time for this transition is 1 (because we assumed $u = 1$).

Similar analysis can be done for second moment of the first-passage times, leading to

$$\langle T_n^2 \rangle = \left(\frac{\partial^2 \widetilde{F}_n(s)}{\partial s^2} \right)_{s=0} = 2 \left[\frac{1 + \sum_{k=0}^{N-n-1} \prod_{j=0}^{k} \frac{\frac{N-n-j}{M}}{n+j+1+\frac{N-n-j-1}{M}}}{\left(n + \frac{N-n}{M}\right)^2} + \frac{\sum_{k=0}^{N-n-1} \left(\prod_{j=0}^{k} \frac{\frac{N-n-j}{M}}{n+j+1+\frac{N-n-j-1}{M}} \sum_{j=0}^{k} \frac{1}{n+j+1+\frac{N-n-j-1}{M}} \right)}{\left(n + \frac{N-n}{M}\right)} \right] \tag{9}$$

Here one can also show that $\langle T_N^2 \rangle = \frac{2}{N^2}$. Note, however, that to obtain mean reaction times and second moment of the reaction times, the quantities that are measured in single-molecule experiments, additional calculations should be done, as we explain below.[20]

Assuming that our system is already in the stationary state, we define P_n as the steady-state probability of finding the system in the effective chemical kinetic state n. Then because the number of the discrete states in the system is finite and the steady state between these effective states will be reached at $t \to \infty$, the following relations can be written for these probabilities (see Figure 1b)[20]

$$\begin{aligned} \frac{N}{M} P_0 &= P_1 \\ \frac{N-1}{M} P_1 &= 2P_2 \\ &\cdots \\ \frac{1}{M} P_{N-1} &= N P_N \end{aligned} \tag{10}$$

Considering the normalization condition, $\sum_{n=0}^{N} P_n = 1$, these equations can be easily solved to obtain the steady-state probabilities[20]

$$P_n(N) = \frac{N!}{(N-n)!n!} \frac{x^n}{(1+x)^N} \tag{11}$$

where $x = \frac{1}{M}$.

We are interested in evaluating the mean reaction (catalytic turnover) times for chemical reactions described in Figure 1a that are taking place on the catalysts with N active sites, $\langle \tau \rangle_N$. It is convenient to think about these processes in the way the single-molecule fluorescence experiments are done.[5,7,11,14,15,26,27] Every time the product molecule is formed, a spike in the fluorescence appears. Then the reaction times are the time intervals between two consecutive spikes, and the mean reaction times are measured by averaging over all pairs of intervals between consecutive spikes. In the language of our effective chemical-kinetic model (Figure 1b), the mean reaction time is the properly weighted average over first-passage times from all the states n except the state $n = N$. This is because in the state $n = N$ all active sites are in the conformation CS_M just before making the product and none of the active sites had just produced the molecule P (had a spike in the fluorescent signal), and the reaction cannot start in this kinetic state. As a result, the mean reaction time can be written as

$$\begin{aligned} \langle \tau \rangle_N &= f_0 \langle T_0 \rangle + f_1 \langle T_1 \rangle + f_2 \langle T_2 \rangle + \ldots + f_{N-1} \langle T_{N-1} \rangle \\ &= \sum_{n=0}^{N-1} f_n \langle T_n \rangle = \frac{u+r}{Nru} = \frac{M+1}{Nu} \end{aligned} \tag{12}$$

where $r = u/M$. This important result predicts that the mean reaction times on such heterogeneous catalysts are proportional to the number of intermediates and inversely proportional to the number of active sites.

The coefficient f_n, which is the relative contribution of different effective states n into the reaction time, can be found from

$$f_n = \frac{(N-n)P_n(N)}{\sum_{j=0}^{N} (N-j)P_j(N)} \tag{13}$$

This result can be explained in the following way. In the state n, there are $(N - n)$ active sites which are not in the

https://doi.org/10.1021/acs.jpclett.1c03557
J. Phys. Chem. Lett. 2021, 12, 11802−11810

conformation CS_M, and the catalytic cycle might start at any of them. Then the coefficient f_n is the relative probability for the chemical reaction to start in the state n normalized over all possible starting situations. These relative probabilities can be estimated by substituting eq 11 into eq 13, producing

$$f_n = \frac{(N-1)!}{(N-n-1)!n!}\frac{x^n}{(1+x)^{N-1}} = P_n(N-1) \tag{14}$$

with $f_N = 0$, as expected.

In Figure 3a we present the results for the mean reaction times as the function of the number of active sites N for the fixed number of intermediates M. As expected, the mean reaction times decrease with N because more chemical reactions can take place at more active sites, decreasing the time intervals between successful fluorescence events. Figure 3b shows the mean reaction times as a function of the number of intermediates M for the fixed number of active sites N. Here the mean reaction times increase with the number of intermediates because more intermediate transitions must happen before the product is made. A linear dependence on M is observed because all chemical transitions have the same rates and only the forward steps are considered in these chemical reactions.

Similar analysis can be done for second moment of the reaction times, and we can write

$$\langle \tau^2 \rangle_N = \sum_{n=0}^{N-1} f_n \langle T_n^2 \rangle \tag{15}$$

Together, eqs 11−15 provide an exact analytical description for mean reaction times and for second moment of reaction times for arbitrary sets of parameters.

To understand the molecular mechanisms of complex chemical and biological processes, one frequently utilizes a dimensionless parameter known as the randomness parameter, R.[22,28] This is the quantity that measures the degree of stochastic fluctuations, and it provides the information on the underlying chemical kinetic scheme.[22] The smaller the deviation of this parameter from unity, the smaller the degree of stochastic fluctuations in the system. In addition, $1/R$ gives the bound for the number of rate-limiting chemical states for the sequential kinetic schemes. There are several closely related definitions of this parameter. In this work, we employ the following definition:

$$R_{N,M} = \frac{\langle \tau^2 \rangle_N - \langle \tau \rangle_N^2}{\langle \tau \rangle_N^2} \tag{16}$$

which views the randomness as the normalized variance of the reaction times.

In Figure 4 we present the results of our explicit calculations for the randomness parameters as the function of the number of intermediate chemical states M for variable number of active sites N. In all situations, the dependence is nonmonotonic, starting from $R = 1$ for a noncatalytic reaction with $M = 0$, going through the minimal value at $M = 1$ and then approaching again unity for $M \to \infty$. While the general nonmonotonic behavior is observed in all conditions, increasing the number of active sites decreases the deviation of the randomness from 1, which agrees with the reported experimental trends.[11] The most surprising observation here is that the maximal degree of stochastic fluctuations, measured *via* the normalized variances of the reaction times, is achieved

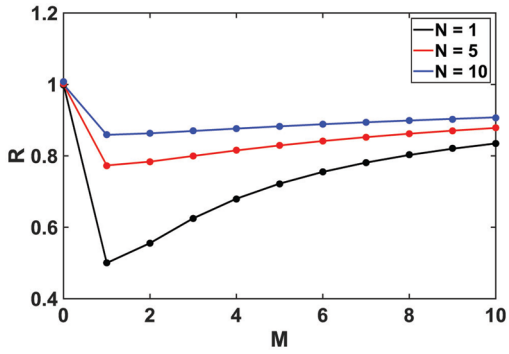

Figure 4. Randomness parameter as a function of the number of intermediate chemical states M for $N = 1$ (black line), $N = 5$ (red line), and $N = 10$ (blue line) active sites. The solid lines are the theoretical predictions, and the symbols are from Monte Carlo simulations.

for the systems with chemical reactions having only one intermediate state ($M = 1$), and adding more intermediates ($M > 1$) decreases the noise, in contrast to naive expectations.

These results can be explained in our simple theoretical model. For $M = 0$, which corresponds to a noncatalytic reaction in the effective chemical kinetic scheme (Figure 1b) only 1 state $n = N$ is possible, *i.e.*, all active sites are always in the state just before making the product. In this case, we have

$$\langle \tau \rangle_N = \langle T_N \rangle = \frac{1}{N}, \quad \langle \tau^2 \rangle_N = \langle T_N^2 \rangle = \frac{2}{N^2} \tag{17}$$

which after substituting into eq 16 gives $R(N, M = 0) = 1$. The randomness parameter is equal to 1 because there is only one effective chemical state in the system. The product molecules can be created in one step from any of the N active sites. In the limit of $M \gg 1$, the system is also mainly found in only one effective chemical state, but this time it corresponds to $n = 0$ (see Figure 1b) because it is almost impossible for any active site to reach the conformation CS_M before the production of molecules P. This again leads to $R(N, M \to \infty) = 1$. For any intermediate values of M, several effective chemical states are possible and the randomness parameter is less than 1, leading to the nonmonotonic behavior shown in Figure 4. However, the system mostly prefers to be found in the states closer to $n = N$ for any $M > 1$. The situation for $M = 1$ corresponds to some kind of the intermediate situation. It is more probable to find the system in the state $n \simeq N/2$, but all other states in the system can also be reached. Because the larger number of chemical states is typically explored for $M = 1$, the randomness parameter deviates in the maximal way from unity, indicating the maximal level of stochastic fluctuations in the reaction times for this case.

The dependence of the randomness parameter on the number of active sites is illustrated in Figure 5. This parameter is always an increasing function of N with $R(N, M) \geq 0.5$ and $R(N \to \infty, M) \to 1$. One can notice that for very large number of active sites ($N \approx 100$) the randomness parameter becomes independent of the number of intermediates M. This suggests that experimental measurements of the randomness can distinguish the mechanisms of underlying chemical reactions only if catalysts have a relatively small number of active sites so that the stochastic effects might show up. These predictions are expected to be valid even for more general mechanisms of catalyzed chemical reactions.

https://doi.org/10.1021/acs.jpclett.1c03557
J. Phys. Chem. Lett. 2021, 12, 11802−11810

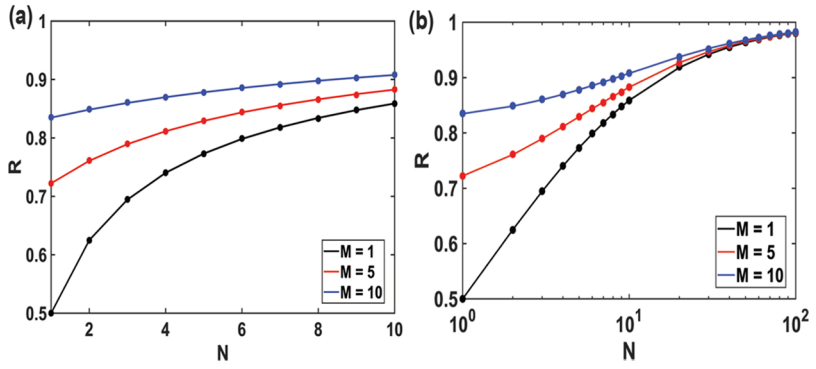

Figure 5. Randomness parameter as a function of the number of active sites for $M = 1$ (black line), $M = 5$ (red line), and $M = 10$ (blue line). (a) Results are shown for $N \leq 10$. (b) Results are shown for $N \leq 100$. The solid lines are the theoretical predictions and the symbols are from Monte Carlo simulations.

We can explain these observations because our theoretical approach gives us the analytical solutions for all dynamic properties. For $N = 1$ active site, only two chemical states, $n = 0$ and $n = 1$, are possible. Then one can obtain from eqs 8 and 9

$$\langle T_0 \rangle = (M + 1), \quad \langle T_1 \rangle = 1 \tag{18}$$

and

$$\langle T_0^2 \rangle = 2(M^2 + M + 1), \quad \langle T_1^2 \rangle = 2 \tag{19}$$

From eq 13, we derive $f_0 = 1$, and this gives us

$$\langle \tau \rangle_1 = \langle T_0 \rangle = (M + 1),$$
$$\langle \tau^2 \rangle_1 = \langle T_0^2 \rangle = 2(M^2 + M + 1) \tag{20}$$

Substituting this into eq 16 finally leads to

$$R(1, M) = \frac{M^2 + 1}{(M + 1)^2} \tag{21}$$

Thus, for $N = 1$, the randomness parameter is lowest for small number of intermediates, *e.g.*, $R(1, 1) = 0.5$, $R(1, 2) = 0.55$ and $R(1, 3) = 0.625$. For a large number of intermediates, $M \gg 1$, the randomness parameter approaches unity, as explained above.

In the limit of large number of active sites ($N \to \infty$), it can be argued that the stationary distributions of chemical states in our effective scheme is peaking around a specific value n^* which can be found from the condition that

$$\frac{\partial P_n(N)}{\partial n} = 0 \tag{22}$$

at $n = n^*$. Explicit calculations presented in the Supporting Information show that for $N \gg 1$

$$n^* \simeq \frac{N}{M + 1}, \quad P_{n^*}(N \to \infty) \simeq 1 \tag{23}$$

Then, as shown in the Supporting Information, the mean reaction times and the second moment of the reaction times are given by

$$\langle \tau \rangle_N \simeq \frac{M + 1}{N}, \quad \langle \tau^2 \rangle_N \simeq 2\left(\frac{M + 1}{N}\right)^2 \tag{24}$$

Applying these expressions in eq 16 eventually leads to $R(N \to \infty, M) \to 1$.

The main advantage of our theoretical approach is that all dynamic properties can be explicitly evaluated at all conditions, allowing us to explain the physics of the observed phenomena. At the same time, real chemical reactions on catalysts differ from the assumptions made in our model: all transitions are reversible and the rates are not uniform. In addition, more complex topology of chemical reaction pathways can also be observed. This limits the direct application of the simplest model that we presented above for analysis of experimental observations. However, one can argue that our explicit results can be used as bounds in determining the important dynamic features of catalytic processes, providing some important microscopic information. Because our simple model neglected the reverse chemical transitions and assumed that all rates are the same, the calculated catalytic turnover times in our model gives the lowest bound to the actual mean reaction times. Adding the backward steps and making the rates nonuniform should only slow down the processes in the system. Similarly, the calculated randomness parameter provides the upper bound to the parameter that can be measured in experiments because in real systems more stochasticity is expected.

To illustrate the potential application of our theoretical approach, let us consider a recent experimental study on nanoparticle catalysis.[14] In this work, single-molecule fluorescence microscopy has been utilized to investigate the oxidative deacetylation of organic molecules by hydrogen peroxide on gold nanoparticles. It was found that there is a single intermediate in this process, which corresponds to $M = 1$ in our notations. Using the reported distributions of reactions times, we estimated that the lowest randomness parameter value in this system is $R \approx 0.87$. Then, our theory predicts that in the simplest model this would correspond to $N \approx 11$. This means that in those gold nanoparticles there are, at least, 11 active sites where the reaction is taking place. These arguments show how our theoretical method can be applied for a better understanding of real catalytic processes.

Another advantage of our theoretical approach is that it can be extended to more complex chemical reactions. To illustrate this and to understand the role of more complex chemical mechanisms that differ from the simplest sequential scheme in Figure 1a, we consider the chemical reaction that involves reversible branching transitions at all intermediate chemical states.[21,22] At each intermediate state CS_j ($j = 0, 1, ..., M$) of the chemical reaction, a reversible binding transition to the state CS_j^* can occur with ν_1 and ν_2 as the forward and backward transition rates, respectively (see Figure 6a). Note that the $j =$

https://doi.org/10.1021/acs.jpclett.1c03557
J. Phys. Chem. Lett. 2021, 12, 11802−11810

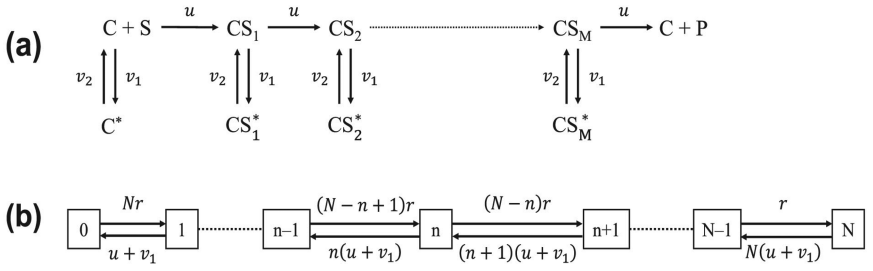

Figure 6. Schematic representations of chemical processes on heterogeneous catalysts with N identical active sites for (a) a branched chemical reaction with M intermediates. (b) Overall effective chemical kinetic scheme for the whole catalyst with the following effective rate constant $r = \frac{u + v_1}{M + (M+1)v_1/v_2}$.

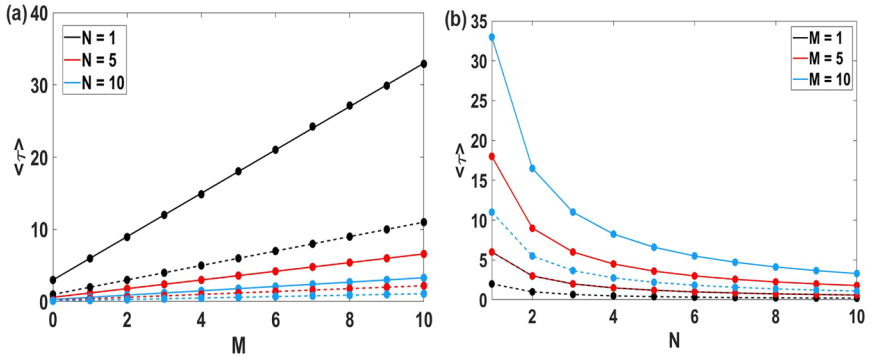

Figure 7. Mean reaction times as a function of (a) the number of intermediate chemical states M for $N = 1$ (black line), $N = 5$ (red line), and $N = 10$ (blue line) active sites and (b) the number of active sites N for $M = 1$ (black line), $M = 5$ (red line), and $M = 10$ (blue line) intermediate chemical conformations for reaction schemes involving branching. The branching transition rates used for calculations are $v_1 = 2\ s^{-1}$ and $v_2 = 1\ s^{-1}$. The solid lines are theoretical predictions for the branching model; the dashed lines are theoretical predictions for the sequential model; and the symbols are from Monte Carlo simulations of corresponding processes.

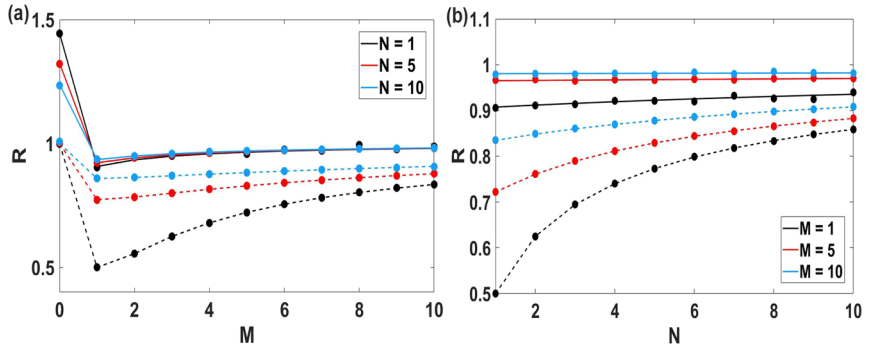

Figure 8. Randomness parameter as a function of (a) the number of intermediates M for $N = 1$ (black line), $N = 5$ (red line) and $N = 10$ (blue line) active sites and (b) the number of active sites N for $M = 1$ (black line), $M = 5$ (red line), and $M = 10$ (blue line) intermediate chemical conformations for reaction schemes involving branching. The branching transition rates used for calculations are $v_1 = 2\ s^{-1}$ and $v_2 = 1\ s^{-1}$. The solid lines are theoretical predictions for the branching model; the dashed lines are theoretical predictions for the sequential model; and the symbols are from Monte Carlo simulations of corresponding processes.

0 case ($CS_0 \equiv C$) describes the empty active site without any substrate, and we also assume that it might be in one of two configurations (CS_0 or CS_0^*). The substrate can bind only when the active site in the conformation CS_0 (Figure 6a). For any active site, the conformation CS_M (before making the final product) can be achieved *via* a series of sequential forward steps that can be occasionally slowed down by reversible branching transitions. One can again build an effective chemical kinetic model with N sequential states, as shown in Figure 6b, but with different effective rate constants $u' = u + v_1$ and r. As explained in the Supporting Information, the effective rate constant r is given by

$$r = \frac{u + v_1}{M + (M+1)v_1/v_2} \tag{25}$$

This means that the same analysis that we developed for the sequential model can be directly applied for the model with reversible branched transitions by proper rescaling of the expressions. This allows us to obtain an explicit description of dynamic properties for catalysis of branched chemical reactions. For example, for the mean reaction times for the branching chemical reactions it can be shown that

$$\langle \tau \rangle_N = \frac{(M+1)(1 + v_1/v_2)}{Nu} \tag{26}$$

https://doi.org/10.1021/acs.jpclett.1c03557
J. Phys. Chem. Lett. 2021, 12, 11802−11810

Figure 7a shows the mean reaction times as a function of the number of intermediates M for the fixed number of active sites N and as a function of the number of active sites N for the fixed number of intermediates M as illustrated in Figure 7b. The behavior of the mean reaction times is similar for both sequential and branching models. But for the fixed values of N and M, the mean reaction times are longer in the system with branching reactions, as expected. This happens because the system can stay longer in those branched intermediate states (CS_j^*) that delay the overall process of reaching the conformation CS_M. As shown in the Supporting Information, using the first-passage time formalism, the higher moments and the randomness parameter can be explicitly calculated for this branching model.

Panels a and b of Figure 8 show the dependence of the randomness parameter R on the number of intermediates and the number of active sites, respectively, for sequential and branching chemical reactions. One can see that the randomness parameter is larger for the reactions with branching at the intermediate states. This corresponds to smaller stochastic fluctuations in the system (R is larger) for the system with the branched reactions. At first, this result seemed to be counterintuitive because in the branched model a larger number of chemical states is explored, and one could expect stronger stochastic fluctuations. To understand this, one might recall that the effective transition rate r (see eq 25) is smaller for the model with branches, at least for the parameters that we are using. This suggests that the system with branching transitions fluctuates less between the effective discrete states (Figure 6b) than the system that follows the sequential mechanism (Figure 1b). This is the reason for smaller fluctuations in the mean reaction times for the system with branching transitions.

We developed a simple theoretical approach to analyze the reaction dynamics of chemical reactions on heterogeneous catalysts with multiple active sites. Our theoretical method is based on a discrete-state stochastic description that allows us to explicitly evaluate dynamic properties of the system *via* stationary-state and first-passage probability density calculations. We investigated two different chemical reaction mechanisms occurring at each active site of the nanocatalyst. Specifically, we concentrated on analyzing the mean reaction times and the randomness parameter that describes the degree of stochastic fluctuations in the underlying chemical processes. It is found that the mean reaction times are proportional to the number of intermediate states (M) and inversely proportional to the number of active sites (N). The effect of varying the parameters N and M is more complex for higher moments of the reaction times. We also found that the randomness parameter, which is a measure of stochastic fluctuations in the system, nonmonotonically depends on the number of intermediates, while it is always increasing with the number of active sites. We predict and explain why the maximal stochastic noise is observed for chemical reactions with only one intermediate state. In addition, when the chemical reactions involve reversible off-pathway branching transitions, the same qualitative behavior as for the model without branches is observed. But both the mean reaction times and the randomness are higher. These observations are explained by the fact that in the branched model more chemical states are visited, increasing the time needed to complete the chemical reaction at the given site. However, the increased randomness for the model with branches corresponds to smaller stochastic fluctuations, which is explained by smaller transition rates between the effective chemical kinetic states of the system. We also suggest that the explicit results for dynamic properties in our theoretical approach can be viewed as bounds for the dynamic properties of the real catalytic systems. Furthermore, the obtained scaling results of dynamic properties as the function of number of active sites or number of intermediates are expected to hold for more general chemical reaction mechanisms. We also show explicitly how our theoretical analysis can be applied to obtain the important microscopic information for the underlying chemical processes.

While the presented theoretical model can be fully solved analytically, giving a better understanding of the molecular mechanisms of chemical reactions on catalysts, there are many simplifying assumptions in our model that restrict its direct application for analyzing the experimental data. The model neglects the backward chemical transitions, and it also assumes that all chemical transition rates are the same. It will be important to generalize this simple approach to make it more realistic while still being able to solve it explicitly because this provides a better understanding of the microscopic picture in catalytic reactions. Testing the scaling predictions with various experimental methods will be also an important step in clarifying the complex mechanisms of chemical reactions on heterogeneous catalysts.

■ ASSOCIATED CONTENT

Supporting Information

The Supporting Information is available free of charge at https://pubs.acs.org/doi/10.1021/acs.jpclett.1c03557.

Specific calculations on randomness parameter in the limit of a large number of active sites, mean reaction time, and randomness parameter for the branching model (PDF)

■ AUTHOR INFORMATION

Corresponding Authors

Srabanti Chaudhury − *Department of Chemistry, Indian Institute of Science Education and Research, Pune 411008 Maharashtra, India;* orcid.org/0000-0001-6718-8886; Email: srabanti@iiserpune.ac.in

A. B. Kolomeisky − *Department of Chemistry and Center for Theoretical Biological Physics, Department of Chemical and Biomolecular Engineering, Department of Physics and Astronomy, Rice University, Houston, Texas 77005-1892, United States;* orcid.org/0000-0001-5677-6690; Email: tolya@rice.edu

Author

Bhawakshi Punia − *Department of Chemistry, Indian Institute of Science Education and Research, Pune 411008 Maharashtra, India*

Complete contact information is available at: https://pubs.acs.org/10.1021/acs.jpclett.1c03557

Author Contributions

[§]Both A.B.K. and S.C. are corresponding authors and have contributed equally to this work.

Notes

The authors declare no competing financial interest.

https://doi.org/10.1021/acs.jpclett.1c03557
J. Phys. Chem. Lett. 2021, 12, 11802−11810

■ ACKNOWLEDGMENTS

B.P. acknowledges the Prime Minister Research Fellowship (PMRF), India, for funding and fellowship. S.C. acknowledges the support from SERB, India (CRG/2019/000 515). A.B.K. acknowledges the support from the Welch Foundation (C-1559), from the NSF (CHE-1953 453 and MCB-1941 106), and from the Center for Theoretical Biological Physics sponsored by the NSF (PHY-2019 745). We also thank H. Shen and P. Chen for sharing with us experimental data and for useful discussions.

■ REFERENCES

(1) Somorjai, G. A.; Li, Y. *Introduction to Surface Chemistry and Catalysis*; John Wiley & Sons: New York, 2010.
(2) Ross, J. R. *Heterogeneous Catalysis: Fundamentals and Applications*; Elsevier: Amsterdam, The Netherlands, 2011.
(3) Friend, C. M.; Xu, B. Heterogeneous Catalysis: A Central Science for a Sustainable Future. *Acc. Chem. Res.* **2017**, *50*, 517−521.
(4) Zhang, Z.; Zandkarimi, B.; Alexandrova, A. N. Ensembles of Metastable States Govern Heterogeneous Catalysis on Dynamic Interfaces. *Acc. Chem. Res.* **2020**, *53*, 447−458.
(5) Chen, P.; Zhou, X.; Andoy, N. M.; Han, K.-S.; Choudhary, E.; Zou, N.; Chen, G.; Shen, H. Spatiotemporal Catalytic Dynamics within Single Nanocatalysts Revealed by Single-Molecule Microscopy. *Chem. Soc. Rev.* **2014**, *43*, 1107−1117.
(6) Makarov, D. E. *Single Molecule Science: Physical Principles and Models*; CRC Press, 2015.
(7) Xu, W.; Kong, J. S.; Yeh, Y. E.; Chen, P. Single-Molecule Nanocatalysis Reveals Heterogeneous Reaction Pathways and Catalytic Dynamics. *Nat. Mater.* **2008**, *7*, 992−996.
(8) Xu, W.; Kong, S.; Chen, P. Probing the Catalytic Activity and Heterogeneity of Au-Nanoparticles at the Single-Molecule Level. *Phys. Chem. Chem. Phys.* **2009**, *11*, 2767−2778.
(9) Ochoa, M. A.; Chen, P.; Loring, R. F. Single Turnover Measurements of Nanoparticle Catalysis Analyzed with Dwell Time Correlation Functions and Constrained Mean Dwell Times. *J. Phys. Chem. C* **2013**, *117*, 19074−19081.
(10) Burda, C.; Chen, X.; Narayanan, R.; El-Sayed, M. A. Chemistry and Properties of Nanocrystals of Different Shapes. *Chem. Rev.* **2005**, *105*, 1025−1102.
(11) Zhou, X.; Xu, W.; Liu, G.; Panda, D.; Chen, P. Size Dependent Catalytic Activity and Dynamics of Gold Nanoparticles at the Single-Molecule Level. *J. Am. Chem. Soc.* **2010**, *132*, 138−146.
(12) Lu, H.; Xun, L.; Xie, X. S. Single-Molecule Enzymatic Dynamics. *Science* **1998**, *282*, 1877−1882.
(13) English, B. P.; Min, W.; van Oijen, A. M.; Lee, K. T.; Luo, G.; Sun, H.; Cherayil, B. J.; Kou, S. C.; Xie, X. S. Ever-Fluctuating Single Enzyme Molecules: Michaelis Menten Equation Revisited. *Nat. Chem. Biol.* **2006**, *2*, 87−92.
(14) Shen, H.; Zhou, X.; Zou, N.; Chen, P. Single-Molecule Kinetics Reveals a Hidden Surface Reaction Intermediate in Single-Nanoparticle Catalysis. *J. Phys. Chem. C* **2014**, *118*, 26902−26911.
(15) Xu, W.; Kong, S.; Chen, P. Single-Molecule Kinetic Theory of Heterogeneous and Enzyme Catalysis. *J. Phys. Chem. C* **2009**, *113*, 2393−2404.
(16) Chaudhury, S.; Cao, J.; Sinitsyn, N. A. Universality of Poisson Indicator and Fano Factor of Transport Event Statistics in Ion Channels and Enzyme Kinetics. *J. Phys. Chem. B* **2013**, *117*, 503−509.
(17) Chaudhury, S. Poisson Indicator and Fano Factor for Probing Dynamic Disorder in Single-Molecule Enzyme Inhibition Kinetics. *J. Phys. Chem. B* **2014**, *118*, 10405−10412.
(18) Das, A.; Chaudhury, S. Modeling the Heterogeneous Catalytic Activity of a Single Nanoparticle Using a First Passage Time Distribution Formalism. *Chem. Phys. Lett.* **2015**, *641*, 193−198.
(19) Singh, D.; Chaudhury, S. A Stochastic Theoretical Approach to Study the Size-Dependent Catalytic Activity of a Metal Nanoparticle at the Single Molecule Level. *Phys. Chem. Chem. Phys.* **2017**, *19*, 8889−8895.
(20) Chaudhury, S.; Singh, D.; Kolomeisky, A. B. Theoretical Investigations of the Dynamics of Chemical Reactions on Nanocatalysts with Multiple Active Sites. *J. Phys. Chem. Lett.* **2020**, *11*, 2330−2335.
(21) Kolomeisky, A. B.; Fisher, M. E. Periodic Sequential Kinetic Models with Jumping, Branching and Deaths. *Phys. A* **2000**, *279*, 1−20.
(22) Kolomeisky, A. B. *Motor Proteins and Molecular Motors*; CRC Press: New York, 2015.
(23) Metzler, R.; Oshanin, G.; Redner, S. *First-Passage Phenomena and Their Applications*; 2014.
(24) van Kampen, N. G. *Stochastic Processes in Physics and Chemistry*; Elsevier, 1992; Vol. *1*.
(25) Redner, S. *A Guide to First-Passage Processes*; Cambridge University Press, 2001.
(26) Xu, W.; Shen, H.; Liu, G.; Chen, P. Chemistry and Properties of Nanocrystals of Different Shapes. *Nano Res.* **2009**, *2*, 911−922.
(27) Ye, R.; Mao, X.; Sun, X.; Chen, P. Analogy between Enzyme and Nanoparticle Catalysis: A Single-Molecule Perspective. *ACS Catal.* **2019**, *9*, 1985−1992.
(28) Yang, S.; Cao, J.; Silbey, R. J.; Sung, J. Quantitative Interpretation of the Randomness in Single Enzyme Turnover Times. *Biophys. J.* **2011**, *101*, 519−524.

https://doi.org/10.1021/acs.jpclett.1c03557
J. Phys. Chem. Lett. 2021, 12, 11802−11810